Fundamental Limits on Beam Stability at the Advanced Photon Source

Glenn Decker, John Carwardine, Om Singh

Advanced Photon Source, Argonne National Laboratory, 9700 South Cass Avenue, Argonne, IL 60439 USA

Abstract. Orbit correction is now routinely performed at the few-micron level in the Advanced Photon Source (APS) storage ring. Three diagnostics are presently in use to measure and control both AC and DC orbit motions: broad-band turn-by-turn rf beam position monitors (BPMs), narrow-band switched heterodyne receivers, and photoemission-style x-ray beam position monitors. Each type of diagnostic has its own set of systematic error effects that place limits on the ultimate pointing stability of x-ray beams supplied to users at the APS. Limiting sources of beam motion at present are magnet power supply noise, girder vibration, and thermal timescale vacuum chamber and girder motion. This paper will investigate the present limitations on orbit correction, and will delve into the upgrades necessary to achieve true submicron beam stability.

INTRODUCTION: POWER SPECTRAL DENSITY

An essential tool in the study of beam stabilization is the power spectral density. Simply put, the power spectral density is the mean square signal per unit frequency, whether the signal is measured in volts, microns, or furlongs per fortnight. Upon integration (or summation) over the available frequency band represented in a given data set, one arrives at the mean square signal in that band, the square root of which yields the rms signal. Shown in Eqs. (1) is the definition of a discrete Fourier transform pair for a time-sampled data set $\{x_n\}$ containing N samples, while Eq. (2) is a statement derived from Parseval's theorem, forming the basis for the definition of power spectral density [1]:

$$X_k \equiv \frac{1}{N}\sum_{n=0}^{N-1} x_n e^{2\pi i n k/N} \quad , \qquad x_n = \sum_{k=0}^{N-1} X_k e^{-2\pi i n k/N} \quad , \tag{1}$$

$$\sigma_x^2 \equiv \frac{1}{N}\sum_{n=0}^{N-1} (x_n - \langle x\rangle)^2 = \langle x^2\rangle - \langle x\rangle^2 = \sum_{k=1}^{N-1} |X_k|^2 \quad ; \quad \left(\langle x\rangle \equiv \frac{1}{N}\sum_{n=0}^{N-1} x_n\right) \quad . \tag{2}$$

The key point to notice in Eq. (2) is that the sums, whether taken in frequency or time domain, produce an invariant quantity, namely the mean square signal amplitude. The k=0 component of the sum over frequency (i.e., k) in Eq. (2) has been moved to the

DISCLAIMER

left-hand side of the equation and is none other than the square of the mean, or D.C. value for the data set $\{x_n\}$, as can easily be verified by inserting k = 0 into the first of Eqs. (1). Power spectral density is quantitatively defined to be $2\,|X_k|^2/\delta f$, (k = 0...N/2), where $\delta f = 1/(N\,\delta t)$ is the frequency discretization interval, δt is the sampling period, and N is the number of samples. Values of $|X_k|$ from k = N/2+1 to N-1 are just a mirror image of those from k = 1 to N/2−1, explaining the factor of 2. "Integrating" the power spectral density from zero up the the Nyquist frequency $f_{Ny} = (N/2)\delta f = 1/(2\delta t)$ yields the mean square signal defined in Eq. (2).

One impediment to the understanding of spectra displayed in other than power spectral density units is the fact that one must carefully account for the sampling rate and duration in order to be able to infer rms noise amplitude. For example, a plot of peak FFT amplitude vs. frequency, while convenient for picking off the amplitude of a pure sine wave, can be difficult to interpret in the case of purely random noise. A white noise source with constant power spectral density P volts^2/Hz, for example, corresponds to a signal having an rms amplitude of simply $(P\,\Delta f)^{1/2}$, where Δf is the frequency band of interest, measured in Hz. In the context of beam stability, a useful measure for power spectral density is (mm^2/Hz).

Keep in mind that information is unavoidably discarded when a continuous signal is sampled at discrete time intervals. In particular, changes in a continuously variable quantity, i.e., $x(t)$, that occur more rapidly than the sample period δt will be "aliased" [1] to lower frequencies when the variable is represented as a set of discrete numbers $x_n = x(n\,\delta t)$. In spite of this, Eq. (2) will provide an accurate value for the rms noise in the continuous signal $x(t)$ provided the number of samples N is large enough even though the shape of the spectrum X_k vs. k will not be an accurate representation of the spectrum of $x(t)$.

SOURCES OF BEAM MOTION

Shown in Table 1 are the quantities of rms beam motion contained in four frequency bands: 10^{-6} to 0.017 Hz (drift), 0.017 to 30 Hz (jitter), 30 to 500 Hz (high frequency), and 500 Hz to 135 kHz (very high frequency). These numbers must be combined in quadrature to obtain the totals listed in the last row. At the APS, low-frequency drift motion is controlled using workstation-based orbit correction software, while intermediate frequency motion (jitter) is corrected using real time digital feedback operating at a 1 kHz update rate [2]. Correction bandwidth presently extends to about 50 Hz. The dominant sources of beam motion are indicated in the table for each frequency band.

Shown in Figure 1 is a plot of beam position power spectral density, averaged over the forty zero-dispersion straight sections at the APS, corresponding to the locations of insertion devices (IDs) (35 of the forty are available for IDs, the other five are used for injection and rf hardware).

TABLE 1. Beam Stability Performance to Date (5/98)

Frequency Band	Horizontal Motion ΔX (microns rms)	Vertical Motion ΔY (microns rms)	Limitations
Low-frequency drift (10^{-6} - 0.017 Hz)	$< \sigma_x^*$	2.5 to 20	BPM electronics intensity dependence, mechanical and electrical thermal effects, rf BPM bunch pattern dependence, ID x-BPM stray radiation
Jitter (0.017 - 30 Hz)	< 4.5, or 1.3% σ_x^*	< 1.8, or 10% σ_y^*	High bandwidth corrector availability, power supply stability, ID x-BPM stray radiation
High frequency (30 - 500 Hz)	< 12.4	< 7.5	Power supply stability rf voltage stability
Very high frequency (0.5 - 135 kHz)	5	6	rf voltage stability, multibunch Instabilities
Broadband TOTAL	14.1 + drift	10.1 to 22.3	Long-term drift

* Beam sizes σ_x = 335 microns, σ_y = 18 microns @ 1% coupling

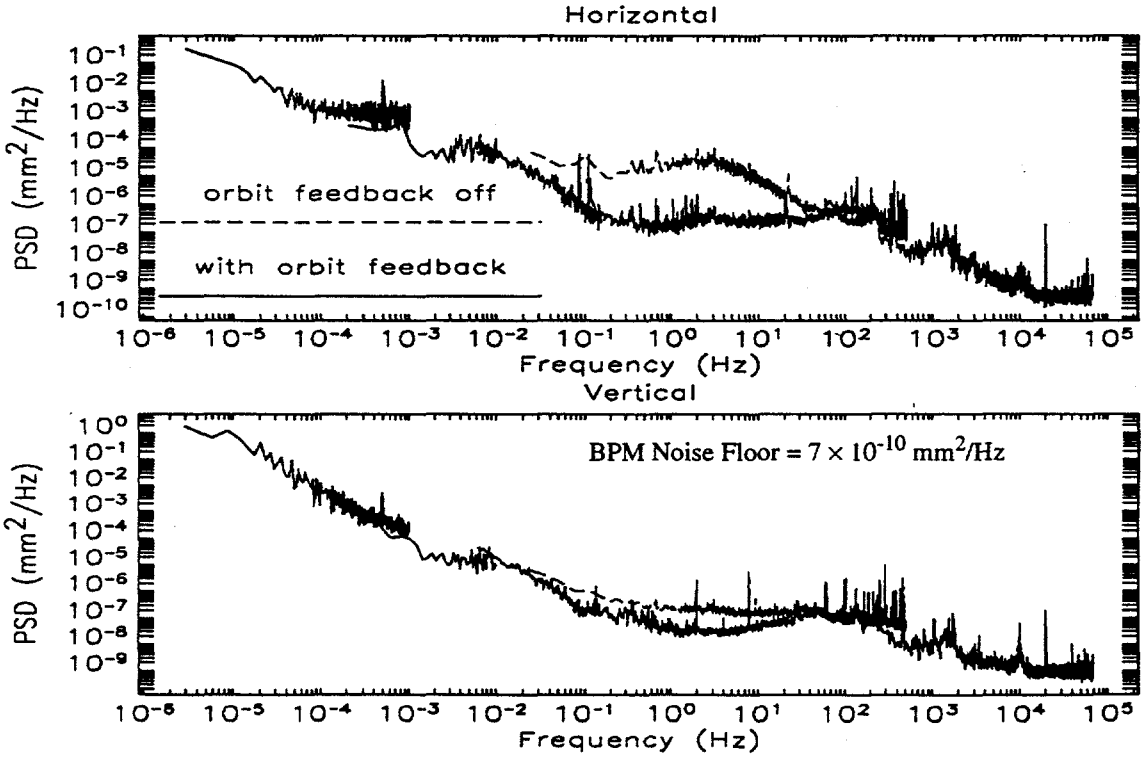

FIGURE 1. Horizontal and vertical APS beam motion power spectral densities.

This plot shows ten decades of frequency, extending from effects occurring on a turn-by-turn basis down to long-term drift effects of several days. The data shown was acquired using the same diagnostic, namely the broadband rf BPM system [3] that employs amplitude-to-phase conversion of 100-ns-long, 352-MHz tone bursts deriving from individual bunches, and sampled on a turn-by-turn basis (270-kHz sampling rate).

Features to note are a spectral line at approximately 5×10^{-4} Hz, corresponding to a one-half hour water temperature cycle, and two lines near 10^{-1} Hz, one caused by the "DC" orbit corrections that occur every ten seconds or so and a second caused by the BPM intensity-dependent offset correction that occurs in the same time frame. A significant bump occurs in the open-loop horizontal motion, centered about 1 or 2 Hz, that is caused principally by power supply rumble, ground motion, and other electromagnetic interference. The thick aluminum vacuum chamber provides an excellent shield from stray electromagnetic fields above a few Hz. Vertical spectral lines at 2, 4, and 8 Hz are the result of the injector synchrotron's 2-Hz duty cycle. The synchrotron tune generally lies near 1.7 kHz and is observable in the horizontal plane. All of the storage ring power supplies except the main dipole are powered independently by pulse-width-modulated DC-DC converters that switch at a 20-kHz rate. The resulting 20 kHz spectral line and harmonics at 40 and 60 kHz are easily identified; however, they are most likely picked up in the BPM data acquisition stage and largely do not correspond to real beam motion. Although not apparent in Figure 1, if one were to show the horizontal spectrum measured at a high dispersion point in the lattice, a spectral line at 360 Hz and harmonics thereof would be seen coming directly from the rf system high-voltage power supplies that cause amplitude and phase ripple, inducing energy oscillations.

BEAM POSITION MEASUREMENT LIMITATIONS

Aliasing

The primary diagnostic used for orbit measurement and control is the monopulse receiver system that records turn-by-turn information and provides hardware averaging (up to 2048 samples to EPICS, 32 turns for feedback). This averaging is presently a "fundamental performance limitation." Data is sampled on every turn, alternating between horizontal and vertical, yielding an effective sample rate of 135.8 kHz in each plane, i.e., half the APS revolution frequency. Thus the available bandwidth on a single turn is the Nyquist frequency, about 68 kHz. The bandwidth available at the output to the 2048-sample "boxcar averager" is thus 68 kHz/2048 = 33.1 Hz; out of the 32-sample averager it is 2.1 kHz. The maximum realistic sampling rate supported by the EPICS controls system is 10 Hz, meaning that a significant aliasing problem exists. A similar issue is present for the feedback system that was originally intended to operate at a 4-kHz rate but is presently sampling at 1 kHz. Thus everything between the 500-Hz feedback sampling Nyquist frequency and the 2.1-kHz signal bandwidth gets aliased down below 500 Hz. An upgrade to the digital processing is in the works that will eliminate these aliasing issues for both the real-time and EPICS sampling rates.

Noise Floor

A careful measurement indicates that the monopulse receivers generate the equivalent of about 7 microns of rms noise on a single measurement, i.e., in a 68-kHz bandwidth. Since this noise scales as the square root of bandwidth, an equivalent statement is that the BPM noise floor is about 27 nanometers/$\sqrt{\text{Hz}}$, or 7.3×10^{-10} mm^2/Hz (see Fig. 1). It is desirable for the beam to be stable to within about 5% of its size, and since the vertical beam size with 1% coupling is about 20 microns rms, the tightest stability specification at the APS presently is 1 micron rms. Based on the noise-floor measurements, we are able to measure this level of motion in bandwidths of 1.4 kHz or less, another fundamental limit. Motion faster than a few tens of Hz for most x-ray experimenters appears as an effective small increase in beam size. They are thus more tolerant of beam motions in this band provided that the effective beam size is stable at lower frequencies.

Intensity and Bunch Pattern Dependence

While the noise floor dictates the high-frequency performance of the the monopulse receivers, more serious limitations occur at very low frequencies as a result of systematic intensity dependence. As the beam decays, position monitor readbacks have been found to vary by some tens of microns in the absence of real beam motion. The effect can be modelled as an intensity-dependent offset and is quantified at the beginning of each operational period. Corrections are calculated and applied as the beam current decays. Reproducibility of this effect is at best a few microns, giving another stability limitation.

Another serious effect is a sensitivity of the monopulse system to changes in fill pattern. The APS injectors provide single pulses at a 2-Hz rate, and the timing system is adjusted to direct the injected bunch at different buckets as a fill proceeds, resulting in small changes in fill pattern from one fill to the next as injection efficiency varies. An upgrade to the monopulse system's rf front end is underway to address this issue [3].

To overcome both the intensity and bunch pattern dependence, new electronics based on narrow-band switched heterodyne receivers [4] have been purchased and are undergoing early commissioning. These receivers are to be placed immediately upstream and downstream of all insertion device x-ray source points, with pickup electrodes fixed to the small-aperture vacuum chambers (most have an 8-mm vertical full aperture). These small-aperture chambers result in position sensitivity that is greater than for the standard vacuum chambers by a factor of 3 vertically and 6 horizontally. If the electronics described in Ref. 4 indeed achieve micron-scale resolution as stated with a 40-mm aperture chamber similar to the standard APS chamber, then in principle at least, long-term stability at the 100- to 300-nanometer rms scale should be attainable (relative to the vacuum chamber location, of course).

MECHANICAL STABILITY

In spite of the potential for beam position monitor electronics to detect submicron beam motions, the lack of an absolute mechanical datum and mechanical component stability dominate our ability to stabilize the orbit at very low frequencies. For example, our small-aperture insertion device vacuum chambers are rigidly supported 1.4 meters above the floor. The air and water temperature in the tunnel is generally stabilized to within ± 0.3 °C rms. Given that thermal expansion coefficients tend to be on the order of 1×10^{-5}, this translates into a vertical chamber motion of order $1.4 \times 0.3 \times 1 \times 10^{-5} =$ 4.2 microns rms. This will almost always be the case; mechanical components typically cannot be stabilized to better than 5 to 10 microns rms owing to one's ability to regulate temperature. Worse yet, as the beam is injected and decays away, the thermal load on water cooling systems varies and vacuum chamber shape distortions inevitably result [5]. Chamber motions at the APS are typically smaller than ± 2 microns, a consequence of careful masking of all vacuum chamber surfaces by discrete water-cooled radiation absorbers.

Another source of beam motion is associated with mechanical component vibrations [6]. Typically, ground motion in the APS accelerator enclosure amounts to a few tens of nanometers rms from 2 to 50 Hz, while the magnet motion is in the range of 80 to 100 nanometers rms in the same frequency band. This is not yet a limiting source of beam motion since power supply noise dominates at these frequencies.

X-RAY BEAM POSITION MONITORS

One significant exception to the limitation on mechanical stability is the support structure for the x-ray BPM (x-BPM) photoemission blade monitors [7] where special attention has been given to thermal insulation and vibration damping. The x-ray BPMs are placed inside the accelerator enclosure, some 15 to 20 meters from the x-ray source points, with two units installed for each beamline. On bending magnet beamlines a two-blade design is used with one upper and one lower blade for vertical position detection only. The insertion device beamlines employ four-blade designs, with the blades arranged in such a manner that the upstream set of blades does not cast shadows on the downstream unit's blades. The electronics presently in use consist of a set of micro-ammeters, the outputs of which are processed to generate delta over sum-type position signals. The bending magnet x-BPMs, owing to their superior mechanical support design and simple radiation geometry, provide the

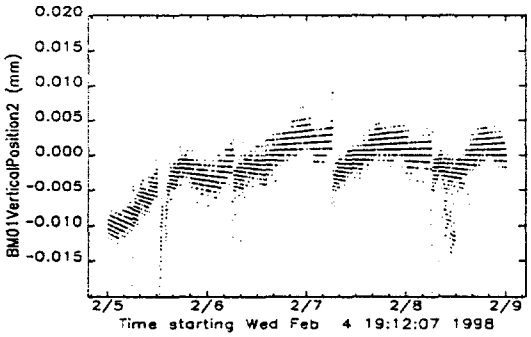

FIGURE 2. Bending magnet x-BPM data.

most believable data on long-term vertical beam stability. Shown in Figure 2 is a set of data, collected over a (good) four-day period, indicating vertical beam motion of ± 2.7 microns rms.

The insertion device x-ray BPMs, although similar mechanically and electrically to their bending magnet counterparts, have some critical differences that complicate their use. The most important difference is that the radiation travelling along the beamline is composed not only of the insertion device photons of interest, but also of stray radiation emanating from upstream and downstream dipole magnet fringe fields, from steering correctors, and from sextupoles and quadrupoles with offset trajectories. The effect of the stray radiation is to induce an offset in the measured ID beam position. Because the relative proportion of stray radiation to insertion device radiation changes when the insertion device gap is varied, an apparent "gap dependent" offset is observed. While significant progress has been made using look-up tables derived from translation stage scans to compensate for this effect [8], performance to date is at the 10- to 20-micron level. This limitation most likely arises from the fact that the stray radiation effects are sensitive to small trajectory changes taking place outside of the insertion device.

A research effort presently underway to address this issue involves the introduction of a chicane into the accelerator lattice to steer the stray radiation away from the x-BPMs (Figure 3). A horizontal parallel translation of the insertion device allows only ID photons and radiation from two nearby correctors to travel down the beamline, simplifying the radiation pattern considerably. Stray radiation is displaced by up to 2 cm horizontally at the x-BPM's location so that it should be easily masked.

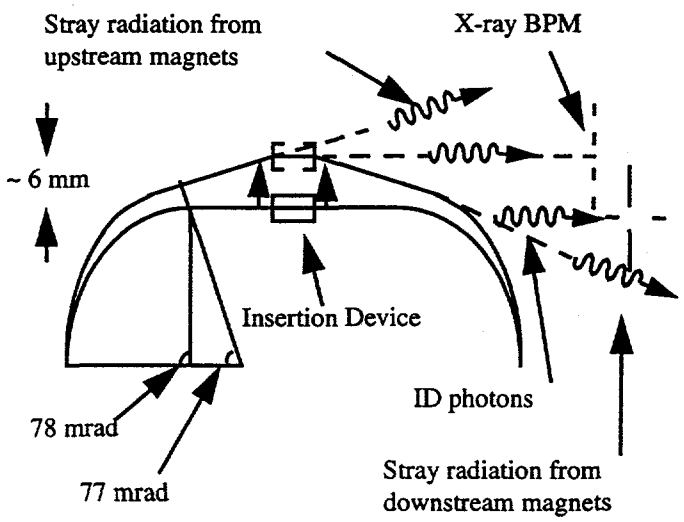

FIGURE 3. Concept to eliminate x-BPM stray radiation.

Orbit Correction Algorithms

The result shown in Figure 2 demonstrates that excellent orbit stabilization is achievable in spite of significant systematic effects such as BPM intensity dependence. The orbit correction algorithm at the APS makes use of as many of the 360 BPMs as possible together with only 80 of the available 317 correctors in each plane. A least-squares algorithm is used to minimize errors detected at the BPMs. This implementation is insensitive to short spatial wavelength (presumed unphysical) orbit motions, such as those caused by intensity dependence, that vary essentially randomly from unit to unit. Additionally, a nonlinear "de-spiking" algorithm is used to replace suddenly misbehav-

ing BPM readbacks by the average of neighboring units, adding to the robustness of the correction.

The alternative to correcting long-wavelength orbit errors is to use so-called "local" control that exactly corrects the orbit at rf BPMs straddling each x-ray source point. The few-micron errors that accumulate over hours or days would result in microradian-scale pointing direction errors with local control. Multiplying by the 20-meter lever arm out to the second x-BPM of Figure 2, this amounts to 20 microns of beam motion instead of the 2.7 microns achieved. The use of an explicitly global correction algorithm that takes advantage of the statistics of having a large number of BPMs is what makes this possible [9]. Local steering for individual beamlines is conducted infrequently and only upon beamline user request.

ACKNOWLEDGEMENTS

The authors would like to thank many individuals in the APS Accelerator Systems Division for their support, including John Galayda, who has always been a strong supporter of beam instrumentation for many years. Michael Borland generated the majority of high-level software necessary to create graphics such as Figure 1, and both he and Louis Emery have spent countless hours in the control room implementing algorithms, the results of which are reported here.

REFERENCES

[1] J. Proakis, D. Manolakis, "Digital Signal Processing," New York, Macmillan Publishing Company (1992).

[2] J. Carwardine, "Real-Time Orbit Feedback at the APS," these proceedings.

[3] R. Lill, "Advanced Photon Source Monopulse RF Beam Position Monitor Front-End Upgrade," these proceedings.

[4] K. Unser, "New Generation Electronics Applied to Beam Position Monitors," Proc. 1996 Beam Instrumentation Workshop, AIP 390, pp. 527-535 (1997).

[5] J. Safranek, O. Singh, L. Solomon, "Orbit Stability Improvement at the NSLS X-ray Ring," Proc. 1995 PAC, IEEE 95CH35843, p. 2711 (1996).

[6] G. Decker, Y. G. Kang, S. Kim, D. Mangra, R. Merl, D. McGhee, S. Sharma, "Reduction of Open-Loop Low Frequency Beam Motion at the APS," Proc. 1995 PAC, IEEE 95CH35843, p. 303 (1996).

[7] D. Shu, J. Barraza, H. Ding, T. M. Kuzay, and M. Ramanathan, "Progress of the APS High Heat Load X-ray Beam Position Monitor Development," Proc. 1997 SRI Conference, AIP CP417, pp. 173-177 (1997).

[8] D. Shu, T.M. Kuzay, "Smart x-ray beam position monitor system for the Advanced Photon Source," Proc. 1997 SRI, Rev. Sci. Instr., **67** (9), p. 3367 (September 1996).

[9] L. Emery, M. Borland, "Advancements in Orbit Drift Correction in the Advanced Photon Source Storage Ring," Proc. 1997 PAC, to be published.